Gravitational wave templates from Extreme Mass Ratio Inspirals

Viktor Skoupý

Institute of Theoretical Physics, Faculty of Mathematics and Physics, Charles University,
Astronomical Institute of the Czech Academy of Sciences

czechLISA, 11 October, 2023

arXiv:2102.04819, arXiv:2201.07044, arXiv:2303.16798

CHARLES UNIVERSITY
Faculty of mathematics
and physics

Astronomical Institute of the Czech Academy of Sciences

Introduction

- Gravitational waves (GWs) detected in 2015
- New era of GW astronomy begun

Introduction

- Gravitational waves (GWs) detected in 2015
- New era of GW astronomy begun

High frequency GWs

- Detected by LIGO-Virgo-KAGRA collaboration
- kHz band
- Compact binary systems, ...

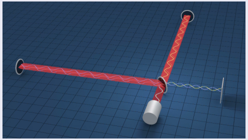

Introduction

- Gravitational waves (GWs) detected in 2015
- New era of GW astronomy begun

High frequency GWs

- Detected by LIGO-Virgo-KAGRA collaboration
- kHz band
- Compact binary systems, ...

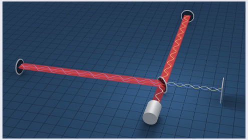

Very low frequency GWs

- Detected by pulsar timing arrays
- nHz band
- Stochastic background from supermassive black hole binaries

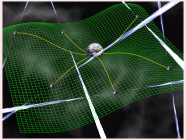

Introduction

- Gravitational waves (GWs) detected in 2015
- New era of GW astronomy begun

High frequency GWs

- Detected by LIGO-Virgo-KAGRA collaboration
- kHz band
- Compact binary systems, . . .

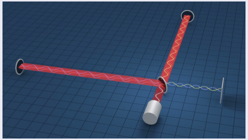

Low frequency GWs

- Detected by future space-based detectors (LISA, . . .)
- mHz band
- Extreme mass ratio inspirals, . . .

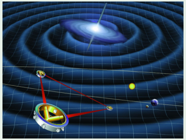

Very low frequency GWs

- Detected by pulsar timing arrays
- nHz band
- Stochastic background from supermassive black hole binaries

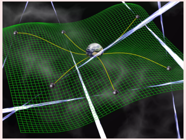

Extreme mass ratio inspirals

- Stellar-mass compact object orbiting a massive black hole
- Mass ratio $q = \mu/M$ between 10^{-7} and 10^{-4}
- Energy and angular momentum loss due to gravitational radiation reaction
- Secondary body completes 10^4 to 10^5 orbits in the strong field
- GWs emitted to infinity will be possible to detect with LISA
- Opportunity to study strong gravitation around massive black holes
- Signals from EMRIs and other sources will overlap $\Rightarrow$ matched filtering for detection and parameter estimation
- Accurate waveform templates are needed

EMRI modelling

- Spacetime expanded in the mass ratio as $g_{\mu\nu}^{\text{exact}} = g_{\mu\nu} + q h_{\mu\nu}^{(1)} + q^2 h_{\mu\nu}^{(2)} + \mathcal{O}(q^3)$
- $h_{\mu\nu}^{(n)}$ calculated from expanded Einstein equations
- Two timescale approximation

$$\Phi = \frac{1}{q}\Phi_0(qt) + \Phi_1(qt) + \mathcal{O}(q)$$

- Flux balance laws: the adiabatic term calculated from the asymptotic fluxes
- Effects of the secondary's spin in the postadiabatic term

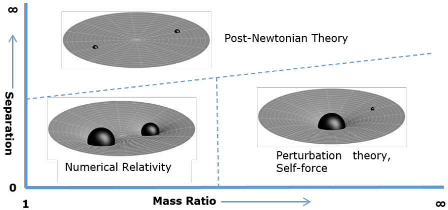

Spinning particle in the Kerr spacetime

- Stress-energy tensor $T^{\mu\nu} = \int \mathrm{d}\tau \left(P^{(\mu} v^{\nu)} \frac{\delta^4}{\sqrt{-g}} - \nabla_\alpha \left(S^{\alpha(\mu} v^{\nu)} \frac{\delta^4}{\sqrt{-g}} \right) \right)$
- Mathisson-Papapetrou-Dixon equations for P^μ and $S^{\mu\nu}$
- Tulczyjew-Dixon SSC $S^{\mu\nu} P_\nu = 0 \Rightarrow$ relation between P^μ and v^μ
- Constants of motion:

Spinning particle in the Kerr spacetime

- Stress-energy tensor $T^{\mu\nu} = \int \mathrm{d}\tau \left(P^{(\mu} v^{\nu)} \frac{\delta^4}{\sqrt{-g}} - \nabla_\alpha \left(S^{\alpha(\mu} v^{\nu)} \frac{\delta^4}{\sqrt{-g}} \right) \right)$
- Mathisson-Papapetrou-Dixon equations for P^μ and $S^{\mu\nu}$
- Tulczyjew-Dixon SSC $S^{\mu\nu} P_\nu = 0 \Rightarrow$ relation between P^μ and v^μ
- Constants of motion:
  - $\mu = \sqrt{-P^\mu P_\mu}$
  - $S = \sqrt{S^{\mu\nu} S_{\mu\nu}/2} = \sigma \mu M$, $\sigma \leq q \ll 1$

Spinning particle in the Kerr spacetime

- Stress-energy tensor $T^{\mu\nu} = \int \mathrm{d}\tau \left(P^{(\mu} v^{\nu)} \frac{\delta^4}{\sqrt{-g}} - \nabla_\alpha \left(S^{\alpha(\mu} v^{\nu)} \frac{\delta^4}{\sqrt{-g}} \right) \right)$
- Mathisson-Papapetrou-Dixon equations for P^μ and $S^{\mu\nu}$
- Tulczyjew-Dixon SSC $S^{\mu\nu} P_\nu = 0 \Rightarrow$ relation between P^μ and v^μ
- Constants of motion:
  - $\mu = \sqrt{-P^\mu P_\mu}$
  - $S = \sqrt{S^{\mu\nu} S_{\mu\nu}}/2 = \sigma \mu M$, $\sigma \leq q \ll 1$
  - $E = -\xi^\mu_{(t)} P_\mu + \xi^{(t)}_{\mu;\nu} S^{\mu\nu}/2$
  - $J_z = \xi^\mu_{(\phi)} P_\mu - \xi^{(\phi)}_{\mu;\nu} S^{\mu\nu}/2$

Spinning particle in the Kerr spacetime

- Stress-energy tensor $T^{\mu\nu} = \int \mathrm{d}\tau \left(P^{(\mu} v^{\nu)} \frac{\delta^4}{\sqrt{-g}} - \nabla_\alpha \left(S^{\alpha(\mu} v^{\nu)} \frac{\delta^4}{\sqrt{-g}} \right) \right)$
- Mathisson-Papapetrou-Dixon equations for P^μ and $S^{\mu\nu}$
- Tulczyjew-Dixon SSC $S^{\mu\nu} P_\nu = 0 \Rightarrow$ relation between P^μ and v^μ
- Constants of motion:
  - $\mu = \sqrt{-P^\mu P_\mu}$
  - $S = \sqrt{S^{\mu\nu} S_{\mu\nu}/2} = \sigma \mu M$, $\sigma \leq q \ll 1$
  - $E = -\xi^\mu_{(t)} P_\mu + \xi^{(t)}_{\mu;\nu} S^{\mu\nu}/2$
  - $J_z = \xi^\mu_{(\phi)} P_\mu - \xi^{(\phi)}_{\mu;\nu} S^{\mu\nu}/2$
  - $C_Y = \sigma_\parallel \sqrt{K} = Y_{\mu\nu} P^\mu S^\nu / (\mu M)$
  - $K_R = K_{\mu\nu} P^\mu P^\nu - 2 P^\mu S^{\rho\sigma} (Y_{\mu\rho;\kappa} Y^\kappa{}_\sigma + Y_{\rho\sigma;\kappa} Y^\kappa{}_\mu)$

Equatorial motion

- Spin parallel to the symmetry axis
- 3 first order ODEs for t, r, ϕ
- Parametrization with p and e

$$r_1 = \frac{pM}{1-e}, \quad r_2 = \frac{pM}{1+e}$$

- Analytic expressions for $E(p,e,\sigma)$, $J_z(p,e,\sigma)$
- Numerical calculation of $\Omega_r(p,e,\sigma)$, $\Omega_\phi(r,e,\sigma)$
- Linearization $f(p,e,\sigma) = f^{(\mathrm{g})}(p,e) + \sigma\delta f(p,e)$ (Skoupý and Lukes-Gerakopoulos [2022])

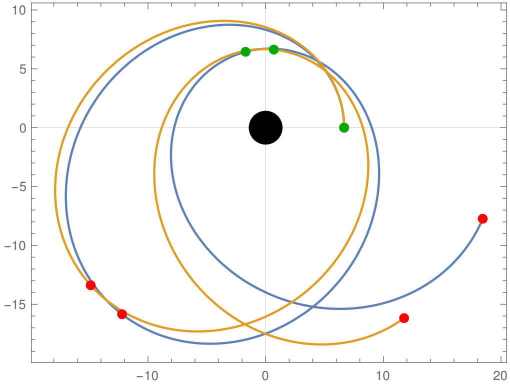

Generic orbits

- Spin vector parallel transported: $\sigma_{\parallel}$ and $\sigma_{\perp}$ parts (Marck [1983])
- Parametrization of the orbit (Drummond and Hughes [2022a,b]):

$$r(\lambda) = \frac{p}{1 + e\cos(\Upsilon_r\lambda + \delta\hat{\chi}_r(\lambda) \qquad\qquad)}$$

$$z(\lambda) = \cos\theta(\lambda) = \sin I \cos\left(\Upsilon_z\lambda + \delta\hat{\chi}_z(\lambda) \qquad\qquad \right)$$

$$u_t(\lambda) = -\hat{E}$$

$$u_\phi(\lambda) = \hat{L}_z$$

Generic orbits

- Spin vector parallel transported: $\sigma_{\parallel}$ and $\sigma_{\perp}$ parts (Marck [1983])
- Parametrization of the orbit (Drummond and Hughes [2022a,b]):

$$r(\lambda) = \frac{p}{1 + e\cos(\Upsilon_r \lambda + \delta\hat{\chi}_r(\lambda) + \delta\chi_r^S(\lambda))} + \mathfrak{r}^S(\lambda)$$

$$z(\lambda) = \cos\theta(\lambda) = \sin I \cos\left(\Upsilon_z \lambda + \delta\hat{\chi}_z(\lambda) + \delta\chi_z^S(\lambda)\right) + \mathfrak{z}^S(\lambda)$$

$$u_t(\lambda) = -\hat{E} + u_t^S(\lambda)$$

$$u_\phi(\lambda) = \hat{L}_z + u_\phi^S(\lambda)$$

Generic orbits

- Spin vector parallel transported: $\sigma_{\parallel}$ and $\sigma_{\perp}$ parts (Marck [1983])
- Parametrization of the orbit (Drummond and Hughes [2022a,b]):

$$r(\lambda) = \frac{p}{1 + e\cos(\Upsilon_r\lambda + \delta\hat{\chi}_r(\lambda) + \delta\chi_r^S(\lambda))} + \mathfrak{r}^S(\lambda)$$

$$z(\lambda) = \cos\theta(\lambda) = \sin I \cos\left(\Upsilon_z\lambda + \delta\hat{\chi}_z(\lambda) + \delta\chi_z^S(\lambda)\right) + \mathfrak{z}^S(\lambda)$$

$$u_t(\lambda) = -\hat{E} + u_t^S(\lambda)$$

$$u_\phi(\lambda) = \hat{L}_z + u_\phi^S(\lambda)$$

- Expansion in Fourier series $f(\lambda) = \sum_{nk} f_{nkj} e^{-in\Upsilon_r\lambda - ik\Upsilon_z\lambda - ij\Upsilon_s\lambda}$
- Phases $w_\mu = \Upsilon_\mu\lambda$ can be used instead of λ
- Fourier coefficients found from a system of linear equations

Teukolsky equation

- Weyl scalar $\psi_4 = -C_{\alpha\beta\gamma\delta} n^\alpha \bar{m}^\beta n^\gamma \bar{m}^\delta$
- Teukolsky equation ${}_{-2}\mathcal{O}_{-2}\psi = 4\pi\Sigma T$

Teukolsky equation

- Weyl scalar $\psi_4 = -C_{\alpha\beta\gamma\delta} n^\alpha \bar{m}^\beta n^\gamma \bar{m}^\delta$
- Teukolsky equation ${}_{-2}\mathcal{O}_{-2}\psi = 4\pi\Sigma T$

Time domain

- (2+1)-D PDE solver `Teukode`
- Horizon-penetrating hyperboloidal coordinates
- Fluxes to future null infinity
- Source term of spinning particle

Teukolsky equation

- Weyl scalar $\psi_4 = -C_{\alpha\beta\gamma\delta} n^\alpha \bar{m}^\beta n^\gamma \bar{m}^\delta$
- Teukolsky equation ${}_{-2}\mathcal{O}\,{}_{-2}\psi = 4\pi\Sigma T$

Time domain

- (2+1)-D PDE solver `Teukode`
- Horizon-penetrating hyperboloidal coordinates
- Fluxes to future null infinity
- Source term of spinning particle

Frequency domain

$$
{}_{-2}\psi = \sum_{l,m} \int \mathrm{d}\omega\, \psi_{lm\omega}(r)\, {}_{-2}S^{a\omega}_{lm}(\theta) e^{-i\omega t + im\varphi}
$$

- Radial equation $\mathcal{D}_{lm\omega}\psi_{lm\omega}(r) = \mathcal{T}_{lm\omega}$
- Angular equation for spin-weighted spheroidal harmonics

Radial Teukolsky equation

- Asymptotic behavior of the radial function

$$\psi_{lm\omega}(r) = \begin{cases} C^{+}_{lm\omega} r^3 e^{i\omega r} & \text{as} \quad r \to \infty \\ C^{-}_{lm\omega} \Delta e^{-ik_H r^*} & \text{as} \quad r \to r_+ \end{cases}$$

- Discrete spectrum of frequencies:

$$C^{\pm}_{lm\omega} = \sum_{n,k,j} C^{\pm}_{lmnkj} \delta(\omega - \omega_{mnkj}), \quad \omega_{mnkj} = m\Omega_\phi + n\Omega_r + k\Omega_z + j\Omega_s$$

$$C^{\pm}_{lmnkj} = \frac{1}{(2\pi)^2 \Gamma} \int \mathrm{d}w_r \mathrm{d}w_z \mathrm{d}w_s I^{\pm}_{lmnkj}(w_r, w_z, w_s) e^{i\omega \Delta t(w_r, w_z, w_s) - im\Delta\phi(w_r, w_z, w_s) + inw_r + ikw_z + ijw_s}$$

- Numerical integration with the midpoint rule, homogeneous solution from the BHPT

Strain and fluxes

- Waveform

$$h = h_+ - ih_\times = -\frac{2}{r}\sum_{lmnkj}\frac{C^+_{lmnkj}}{\omega^2_{mnkj}}S^{a\omega_{mnkj}}_{lm}(\theta)e^{-i\omega_{mnkj}t+im\phi}$$

- Energy and angular momentum fluxes

$$\mathcal{F}^E = \sum_{lmnkj}\frac{\left|C^+_{lmnkj}\right|^2 + \alpha_{lmnkj}\left|C^-_{lmnkj}\right|^2}{4\pi\omega^2_{mnkj}}, \qquad \mathcal{F}^{J_z} = \sum_{lmnkj} m\frac{\left|C^+_{lmnkj}\right|^2 + \alpha_{lmnkj}\left|C^-_{lmnkj}\right|^2}{4\pi\omega^3_{mnkj}}$$

- In linear-in-spin order, fluxes independent of $\sigma_\perp$

Comparison of frequency- and time-domain results

- Equatorial case (Skoupý and Lukes-Gerakopoulos [2021])
- Convergence of the time-domain result to the frequency-domain result for increasing resolution

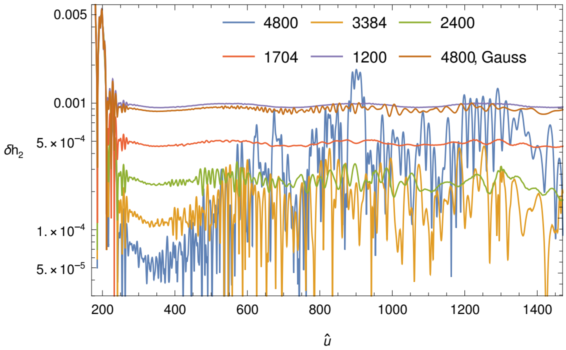

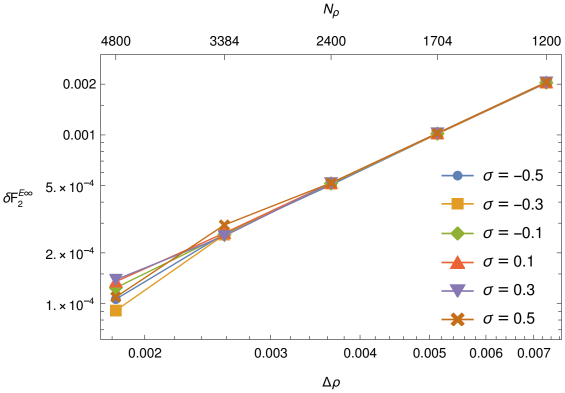

Comparison of frequency- and time-domain results

- Nearly spherical and generic orbits (Skoupý et al. [2023])
- Comparison of linear-in-spin parts of the energy flux

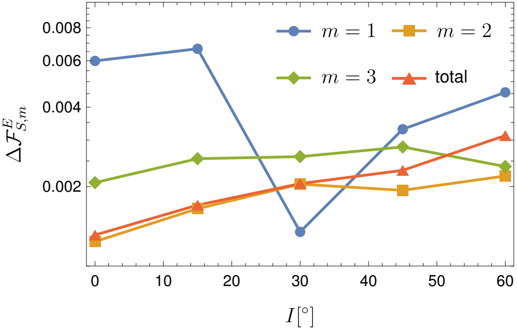

Nearly spherical orbits with $a = 0.9M$, $p = 10$

p	e	$I/^\circ$	m	$\mathcal{F}^E_{S,m}$	$\Delta\mathcal{F}^E_{S,m}$
10	0.1	15	2	-2.8259×10^{-6}	1×10^{-3}
12	0.2	30	1	-1.1954×10^{-7}	2×10^{-5}
12	0.2	30	2	-1.0488×10^{-6}	1×10^{-3}
12	0.2	30	3	-1.4210×10^{-7}	3×10^{-3}
12	0.2	60	2	-8.0550×10^{-7}	5×10^{-4}
15	0.5	15	2	-4.2936×10^{-7}	2×10^{-3}

Generic orbits

Adiabatic inspirals

- Change of orbital parameters for equatorial orbits

$$\frac{\mathrm{d}}{\mathrm{d}t}\begin{pmatrix} p \\ e \end{pmatrix} = \begin{pmatrix} \frac{\partial E}{\partial p} & \frac{\partial E}{\partial e} \\ \frac{\partial J_z}{\partial p} & \frac{\partial J_z}{\partial e} \end{pmatrix}^{-1} \begin{pmatrix} \frac{\mathrm{d}E}{\mathrm{d}t} \\ \frac{\mathrm{d}J_z}{\mathrm{d}t} \end{pmatrix}$$

- Waveform

$$h = -\frac{2}{r}\sum \frac{C^{+}_{lmn}(t)}{\omega^2_{mn}(t)} S^{a\omega_{mn}(t)}_{lm}(\theta) e^{-i\Phi_{mn}(t)+im\phi}$$

- Phase

$$\Phi_{mn}(t) = \int_0^t \omega_{mn}(t')\mathrm{d}t'$$

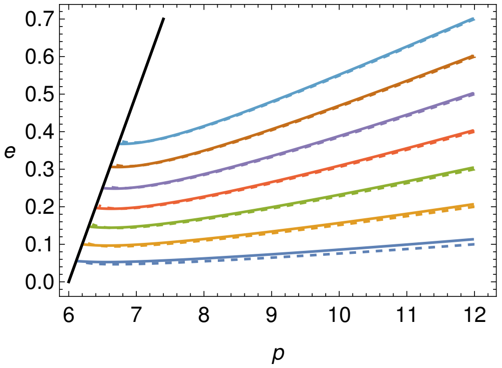

- Linearization: $p(t) = p^{(\mathrm{g})}(t) + \sigma\delta p(t)$, $e(t) = e^{(\mathrm{g})}(t) + \sigma\delta e(t)$
- Phase shift $\delta\Phi_{mn} = n\delta\Phi_r(t) + m\delta\Phi_\phi(t)$

Phase shifts

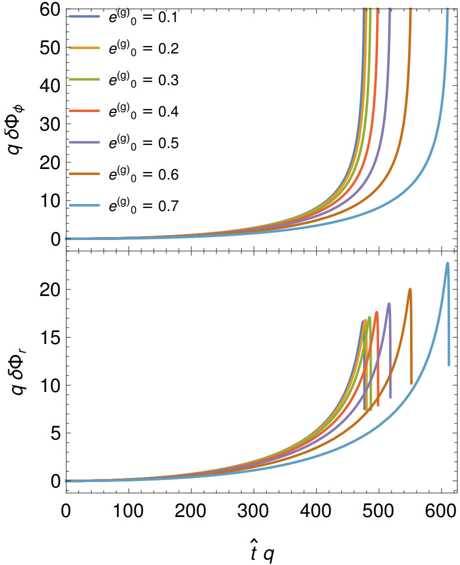

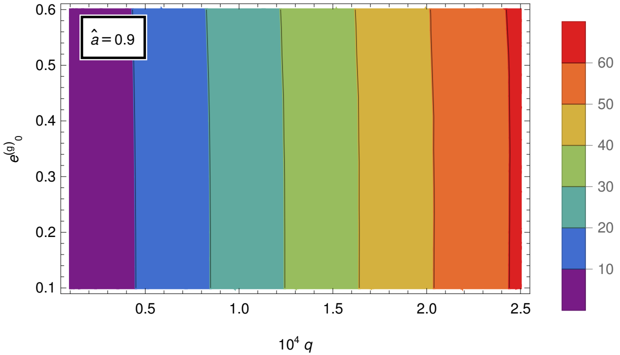

$M = 10^6 M_\odot,\ T = 1\mathrm{yr},\ a = 0.9M$

(Skoupý and Lukes-Gerakopoulos [2022])

Summary

- Secondary spin is needed to model EMRIs
- We calculated the constants of motion and frequencies for equatorial orbits and linearized them in the secondary spin
- Equatorial and generic orbits used to find respective GW fluxes
- We compared GW fluxes calculated in time domain and frequency domain
- We calculated eccentric equatorial inspirals and found spin-induced phase shifts

Thank you

Bibliography

Lisa V. Drummond and Scott A. Hughes. Precisely computing bound orbits of spinning bodies around black holes. I. General framework and results for nearly equatorial orbits. *Phys. Rev. D*, 105(12):124040, June 2022a. doi: 10.1103/PhysRevD.105.12404010.48550/arXiv.2201.13334.

Lisa V. Drummond and Scott A. Hughes. Precisely computing bound orbits of spinning bodies around black holes. II. Generic orbits. *Phys. Rev. D*, 105(12):124041, June 2022b. doi: 10.1103/PhysRevD.105.12404110.48550/arXiv.2201.13335.

J.-A. Marck. Solution to the equations of parallel transport in kerr geometry; tidal tensor. *Proceedings of the Royal Society of London. Series A, Mathematical and Physical Sciences*, 385(1789):431–438, 1983. ISSN 00804630. URL `http://www.jstor.org/stable/2397341`.

Viktor Skoupý and Georgios Lukes-Gerakopoulos. Spinning test body orbiting around a Kerr black hole: Eccentric equatorial orbits and their asymptotic gravitational-wave fluxes. *Phys. Rev. D*, 103(10):104045, May 2021. doi: 10.1103/PhysRevD.103.104045.

Viktor Skoupý and Georgios Lukes-Gerakopoulos. Adiabatic equatorial inspirals of a spinning body into a Kerr black hole. *Phys. Rev. D*, 105(8):084033, April 2022. doi: 10.1103/PhysRevD.105.084033.

Viktor Skoupý, Georgios Lukes-Gerakopoulos, Lisa V. Drummond, and Scott A. Hughes. Asymptotic gravitational-wave fluxes from a spinning test body on generic orbits around a Kerr black hole. *Phys. Rev. D*, 108(4):044041, August 2023. doi: 10.1103/PhysRevD.108.044041.

Images

- Slide 2:
  - T. Pyle/LIGO
  - NASA
  - David Champion/Max Planck Institute for Radio Astronomy
- Slide 4: TimothyRias
- Other: author's own work